IEEE Access
Multidisciplinary ⋮ Rapid Review ⋮ Open Access Journal

Received 29 May 2024, accepted 11 June 2024, date of publication 14 June 2024, date of current version 26 June 2024.
Digital Object Identifier 10.1109/ACCESS.2024.3415015

RESEARCH ARTICLE

A New Constructive Characterization of Stabilizing PID Controllers

CHYI HWANG[1], TZU-CHI WANG[2], FENG-SHENG WANG[1], AND LI-SHIN LU[3]
[1]Department of Chemical Engineering, National Chung Cheng University, Chiayi City 62102, Taiwan
[2]Department of Chemical and Materials Engineering, Chinese Culture University, Taipei 11114, Taiwan
[3]Department of Industrial Engineering and Management, National Quemoy University, Kinmen 89250, Taiwan

Corresponding author: Chyi Hwang (chyihwang@ccu.edu.tw)

This work was supported by the National Science and Technology Council, Taiwan, under Grant NSTC112-2221-E-194-004.

ABSTRACT In this paper, we present a new complete and constructive characterization of all the stabilizing regions in the PID gain space. It is based on D-partition theory and the fact that for a given proportional gain k_p the stability boundaries in the plane of integral and derivative gains are all straight lines. Actually, we present the notion of the critical k_p point, which is defined in the sense that the topology of the D-partition of (k_i, k_d) plane can change when the k_p crosses a critical k_p point. Moreover, we identify seven types of critical k_p points and provide formulas for their computation. With the availability of all critical k_p points, the stabilizing k_p intervals can be exhaustively and exactly determined. By sweeping the k_p parameter over the stabilizing k_p intervals, the whole set of stabilizing PID controllers for a given plant is created. In addition, it allows for an efficient test of the existence of a stabilizing PID controller set without sweeping the k_p parameter. To validate the newly presented analytical and constructive characterization of stabilizing PID controller sets and demonstrate the existence of seven types of critical k_p points, five examples are provided.

INDEX TERMS Stabilizing PID controller set, D-partition theory, parametric-space method, stability domain.

I. INTRODUCTION

As evidenced by the vast amount of research literature on proportional-integral-derivative (PID) controllers, the classical PID control algorithm is still widely applied in a variety of industrial control systems [1], [2], [3], [4], [5]. The main reason for the longstanding use of PID control in various applications is that the principle of the control law is understandable by control engineers, and its control actions provide satisfactory performance for a wide class of processes. Moreover, with the advent of low-cost programmable microprocessors, the implementation and tuning of the PID control algorithm have become advantageous and flexible. Nowadays, the PID control scheme also finds pervasive applications in high-tech industries and products, such as networked control and robots [6], [7], [8].

Despite the advances in modern control synthesis methodologies, such as Youla-Kucera parametrization [9] and Wiener-Hopf spectral factorization method [10], [11], [12], the task of optimal tuning parameters for PID controllers still relies on parametric design methods because a PID controller has only three adjustable gain parameters. Conventional parametric PID design methods rely on graphical approaches, such as Nyquist plot [13], [24], root locus [14], [15], Bode diagram [16], [17], Nichols chart [18], [19], and D-partition theory [20], [21], [22], [23].

The last two decades have witnessed renewed interest in developing new approaches for parametric-space PID design methods. Especially, considerable effort has been devoted to constructing stability/performance feasible domains in the controller parameter space. By searching within these stability/performance feasible domains, the designed PID controllers naturally meet the stability and performance requirements. The regained attention on this research topic by the systems and control researchers can be attributed to the following facts: (i) the stringent performance and stability requirements in control; (ii) the algorithmizations of graphical methods, such as the D-partition technique [22], [23], the Nyquist criterion [13], [24], and generalized Hermite-Biehler Theorem [25]; (iii) the revelation of more structural

The associate editor coordinating the review of this manuscript and approving it for publication was Leimin Wang.

properties of stabilizing PID controller sets [25], [26], [27], [28], [29], [30], [31], such as for a given value of the proportional gain k_p parameter, the stable domain in the (k_i, k_d) plane consists of a finite number of disjoint convex polygons [24], [25], [26], [27], [28], [29], [30], [31].

Since the finding [25] that for a given value of proportional gain k_p the D-partition boundaries in the (k_i, k_d) plane are all straight lines, several research efforts [29], [30], [31], [32], [33], [34], [35], [36], [37], [38], [39], [40], [41] have been devoted to constructing stable regions in the PID parameter space by sweeping the proportional gain k_p. Regarding the efficiency of a method based on the k_p-sweeping approach for the construction of the whole stabilizing PID domain or for the inspection of the existence of stabilizing PID controllers, a particularly crucial task is to assert the so-called stabilizing k_p-intervals within which each k_p guarantees the existence of at least one stable polygon in the (k_i, k_d) plane. However, rather surprisingly, it has seldom been mentioned in the literature, despite the fact that an exact determination of stability will not lead to a conservative stable region or not waste effort in sweeping parameters over unnecessary k_p-intervals. In [25], an effective method was proposed to identify stabilizing k_p-intervals within which the existence of a stable polygon in the (k_i, k_d) plane was guaranteed. An improvement to this method was recently given in [40] by relaxing an unnecessary condition so that the number of stable checks could be reduced. Using the Nyquist stability criterion, Bajcinca [34] derived a necessary condition for discriminating the intervals on the k_p axis over which no stable polygons in the (k_i, k_d) plane exist. However, the use of such conditions can lead to conservative results.

Since stability is the foremost requirement in any control loop design, the stabilizing PID controller set in the gain space is crucial for initiating the optimal tuning process. The availability of the entire stabilizing set of PID controller gains can greatly facilitate optimal PID controller design by eliminating the stability check step in the search process. This is especially important for the multi-objective PID control design case. Therefore, it is essential to have an exact and exhaustive construction of the entire stabilizing PID controllers for a given plant.

The objective of this paper is to show that, to date, the problem of determining exactly the stabilizing k_p-intervals has not been solved thoroughly by presenting a new and complete characterization of the entire set of stabilizing PID controllers for a given plant. More precisely, we identify all seven critical conditions for which any one holds can lead to a change in the topology of the D-partition domains of the PID controller gain space. With these seven types of critical k_p points, an exact and complete characterization of all stabilizing PID can be achieved. The main contributions of this study are as follows:

- It identifies seven types of critical k_p points and analytically characterizes the entire set of stabilizing PID controllers.
- It provides mathematical formulas for calculating all types of critical k_p points for a given plant controlled by a standard PID controller.
- It fully solves the problem of determining exactly and exhaustively the stabilizing k_p-intervals. As a result, the entire set of stabilizing PID controllers for a given plant can be constructed efficiently by sweeping the k_p parameter over all stabilizing k_p-intervals without wasting time in sweeping k_p over non-stabilizing k_p ranges.
- It can now be claimed that the new characterization of all stabilizing PID controllers for a given linear time-invariant system is complete and constructive.

The remainder of this study is organized as follows. In Section II, the basics of D-partition technique are reviewed briefly. In Section III, a new and complete characterization of the D-partition boundaries of the PID controller gain space for a given arbitrary order linear time-invariant system is presented. Section IV presents numerical examples to show that seven types of critical k_p points indeed exist among the systems controlled by the PID controller. Finally, conclusions are presented in Section V.

II. A BRIEF REVIEW OF THE D-PARTITION THEORY

The D-partition theory originated by Neimark [21] and plays a fundamental role in the characterization of stable domains in the parameter space of control systems. It has been widely applied to solve robust stability problems and design lower-order controllers. In particular, the recent progress in constructing an entire set of PID controllers for a given plant is due to a clearer exploration of the topological or geometric properties of the stability domains of the PID controller parameter space. Before presenting our main results, the idea of the D-partition technique is briefly described in this section.

For a continuous-time system with the characteristic polynomial

$$p(s; \boldsymbol{\gamma}) = c_0(\boldsymbol{\gamma}) + c_1(\boldsymbol{\gamma})\, s + c_2(\boldsymbol{\gamma})\, s^2 + \ldots + c_n(\boldsymbol{\gamma})\, s^n \tag{1}$$

where the coefficients $c_i(\boldsymbol{\gamma})$, $i = 0, 1, 2, \ldots n$ are continuous functions of the m parameters $\boldsymbol{\gamma} = (\gamma_1, \gamma_2, \ldots, \gamma_m)$, and the technique of D-partition establishes a direct correspondence between the points in the m-dimensional vector space Γ^m, where γ_i are coordinates, and the number of the left (right) half-plane roots of the polynomial $p(s, \boldsymbol{\gamma})$ in (1). More precisely, using the D-partition technique, the m-space Γ^m of parameters γ_i can be partitioned into domains $D(n_u)$, $n_u = 0, 1, 2, \ldots, n$, which correspond to the polynomial $p(s, \boldsymbol{\gamma})$ having n_u roots with positive real parts. Here, $D(n_u)$, $n_u = 1, 2, \ldots, n$, are referred to as stability domains, and, $D(0)$ is stable domain. It is noted that the domain $D(n_u)$ may be composed of disjoint regions in the m-space. According to the boundary crossing theorem [42], as a point $\boldsymbol{\gamma}$ in the parameter space Γ^m varies continuously across the boundary of two adjacent stability domains, one of the following root

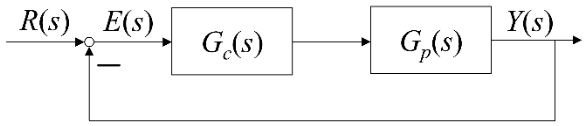

FIGURE 1. A typical unity feedback control system.

movements occurs: (i) a pair of complex conjugate roots of $p(s, \boldsymbol{\gamma})$ moves across the imaginary axis; (ii) a real root moves from one half plane to the other through the origin $s = 0$; and (iii) an infinite root jumps from one half of the plane to the other, corresponding to the characteristic polynomial $p(s, \boldsymbol{\gamma})$ having a degree drop.

Based on the above description of D-partition theory, we see that the power of D-partition theory lies in that it provides a concrete characterization of the stability domain boundaries of the D-partition of the parameter space. For the m-dimensional gain parameter space Γ^m, the D-partition boundaries consist of the following three types of surfaces: (i) real root boundary (RRB) $\partial D_0 : c_0(\boldsymbol{\gamma}) = 0$; (ii) infinite root boundary (IRB) $\partial D_\infty : c_n(\boldsymbol{\gamma}) = 0$; (iii) complex root boundary (CRB) $\partial D_\omega : p(\pm j\omega; \boldsymbol{\gamma})$ for all $\omega \in (0, \infty)$, where $j = \sqrt{-1}$. The CRB is a parametric representation of the boundary surface.

Before leaving the section, it should be mentioned that in the western literature, the D-partition technique also named as D-decomposition technique [43], [44], [45]. In the past, the D-partition method has been applied to analyze graphically the stability of various dynamic systems, including continuous systems [20], [46], discrete systems [47], [48] and nonlinear systems [49], [50], in the two-dimensional parameter plane. Recent advances in D-partition technique include the algorithmization of the method [40], [51] and the robust stability analysis of systems with uncertain parameters [52], [53], [54].

III. THE D-PARTITION OF THE PID GAIN SPACE

Consider the block diagram of a unity feedback control system shown in Fig. 1, where $G_p(s)$ stands for the plant to be controlled, and $G_c(s)$ is the controller. Without a loss of generality, let the transfer function of the plane be

$$G_p(s) = \frac{b_0 + b_1 s + \ldots + b_m s^m}{a_0 + a_1 s + \ldots + a_n s^n} := \frac{B(s)}{A(s)}, m < n \tag{2}$$

and $G_c(s)$ be a PID controller, i.e.,

$$G_c(s) = k_p + \frac{k_i}{s} + k_d s \tag{3}$$

where k_p, k_i, and k_d are the proportional, integral, and derivative gains, respectively, of the PID controller. Throughout this paper, we assume that polynomial $B(s)$ never vanishes for any s on the imaginary axis.

It is well known that the stability investigation of the continuous-time PID control system shown in Fig. 1 involves the root location of the characteristic polynomial

$$p(s; \mathbf{k}) = sA(s) + \left(k_i + k_p s + k_d s^2\right) B(s) \tag{4}$$

where $\mathbf{k} = (k_p, k_i, k_d)$ denotes the PID controller parameter vector. Let $\mathbb{K}$ denote the three-dimensional vector space with k_p, k_i, and k_d as the coordinates, and $\mathbb{K}(n_u)$ the subset of $\mathbb{K}$ for which the characteristic polynomial $p(s; \mathbf{k})$ has n_u roots with positive real parts. Over the past two decades, the D-partition of the parameter space $\mathbb{K}$ associated with characteristic polynomial $p(s; \mathbf{k})$ have received constant attention [20], [21], [22], [23], [55], [56], [57], [58], [59], [60] with a focus on the construction of the entire set $\mathbb{K}(0)$ of stabilizing PID controllers for a given linear time-invariant plant. The interest in exploiting the D-partition technique for PID controller design problems may be ascribed to the finding that the special form of the parameters and k_p, k_i, and k_d entering the coefficients of the characteristic polynomial $p(s; \mathbf{k})$, which for a fixed value of the stability domains in the (k_i, k_d) plane, are convex polygons [25]. In the past two decades, several authors [25], [29], [34], [41] have attempted to solve the problem of exactly and exhaustively determining the stabilizing k_p intervals where for each k_p stable region(s) in the (k_i, k_d) plane is guaranteed to exist. However, as demonstrated below, this problem has not yet been fully resolved. In the following, we present the notion of the critical k_p to reveal all intervals in which the topology of the D-partition of (k_i, k_d) plane remains invariant. The computation of critical k_p values allows for a complete characterization of all stabilizing PID controller set $\mathbb{K}(0)$.

Let ∂D denote the set of D-partition boundaries of the PID parameter space $\mathbb{K}$. This boundary set consists of the following three types of stability boundaries:

$$\text{RRB} : \partial D_0 = \left\{\mathbf{k} \in \mathbb{R}^{\mathbf{3}} : p(0; \mathbf{k}) = 0\right\} \tag{5}$$

$$\text{CRB} : \partial D_\omega = \left\{\mathbf{k} \in \mathbb{R}^{\mathbf{3}} : p(\pm j\omega; \mathbf{k}) = 0 \ \forall \omega \in (0, \infty)\right\} \tag{6}$$

$$\text{IRB} : \partial D_\infty = \left\{\begin{array}{l} \mathbf{k} \in \mathbb{R}^{\mathbf{3}} : q(0; \mathbf{k}) = 0, \\ q(s; \mathbf{k}) = s^n p(1/s; \mathbf{k}) \end{array}\right\} \tag{7}$$

where $q(s; \mathbf{k})$ is the reciprocal polynomial of $p(s; \mathbf{k})$. Here it is worth noting that when the PID parameter point $\mathbf{k}$ moves from one D-partition region into an adjacent region by crossing their common RRB, at least one real root of the characteristic polynomial $p(s; \mathbf{k})$ will move across the imaginary axis of the complex s-plane through the origin $s = 0$. It is also important to note that the IRB ∂D_∞ exists only when one or more PID parameters enter the leading coefficient of characteristic polynomial $p(s; \mathbf{k})$. In such cases, the degree of the polynomial $p(s; \mathbf{k})$ will drop at least by one, and a real root of $p(s; \mathbf{k})$ will jump from $-\infty$ to $+\infty$ or from $+\infty$ to $-\infty$ as the real leading coefficient varies continuously from 0^- to 0^+. Hence, the condition of zero leading coefficient of the polynomial defines the IRB ∂D_∞. Since the polynomial $q(s; \mathbf{k})$ defined in (7) is the reciprocal polynomial of $p(s; \mathbf{k})$, $q(s = 0; \mathbf{k})$ is equivalent to

$p(\pm\infty; \mathbf{k})$. It is mathematically clear to express the condition of zero leading coefficient of $p(s; \mathbf{k})$ by $q(0; \mathbf{k}) = 0$.

According to (5), the equation for describing the boundary ∂D_0 can be obtained simply by setting $s = 0$ in (4), as follows:

$$\partial D_0 : b_0 k_i = 0 \tag{8}$$

Assuming of $b_0 \neq 0$, RRB ∂D_0 is a plane in the three-dimensional gain space $\mathbb{K}$ or a vertical line $k_i = 0$ on the (k_i, k_d) plane. As for the IRB ∂D_∞, it exists when the degree m of $B(s)$ is one less than that of $A(s)$, i.e., $m = n - 1$. In other words, the boundary set ∂D_∞ may be empty, depending on the relative degrees of polynomials $A(s)$ and $B(s)$. Based on its definition given in (7), the boundary ∂D_∞ is characterized by

$$\partial D_\infty: \begin{cases} a_n + k_d b_{n-2} = 0, & \text{if } m = n-1 \\ \emptyset, & \text{otherwise} \end{cases} \tag{9}$$

Next, we consider the characterization of the CRB set ∂D_ω. To this end, we note that the characteristic equation $p(s; \mathbf{k}) = 0$ can be rewritten in the form:

$$k_i + k_p s + k_d s^2 = -\frac{sA(s)}{B(s)} \tag{10}$$

Substituting $s = j\omega$ into the above equation and making rearrangement, we have

$$\left(k_i - k_d\omega^2\right) + jk_p\omega = -\frac{j\omega A(j\omega) B(-j\omega)}{B(j\omega) B(-j\omega)} \tag{11}$$

Because polynomial $B(s)$ is assumed to have no purely imaginary roots, the denominator in (11) never vanishes. Noting that the coefficients of polynomials $A(s)$ and $B(s)$ are real, their real and imaginary decompositions for $s = j\omega$ can be represented as

$$A(j\omega) = A_E\left(\omega^2\right) + j\omega A_O\left(\omega^2\right) \tag{12a}$$

$$B(j\omega) = B_E\left(\omega^2\right) + j\omega B_O\left(\omega^2\right) \tag{12b}$$

Substituting these two decompositions into (11), we obtain the real and imaginary parts of the equation as follows:

$$k_i - uk_d = -\frac{X(u)}{Z(u)} \tag{13a}$$

$$k_p = -\frac{Y(u)}{Z(u)} := f(u) \tag{13b}$$

where $u = \omega^2$ is the squared frequency, and

$$X(u) = u(A_E(u) B_O(u) - A_O(u) B_E(u)) \tag{14a}$$

$$Y(u) = A_E(u) B_E(u) + uA_O(u) B_O(u) \tag{14b}$$

$$Z(u) = B_E(u) B_E(u) + uB_O(u) B_O(u) \tag{14c}$$

Let $F\left(u; k_p\right)$ be the k_p-parametrized u-polynomial defined as

$$F\left(u; k_p\right) = Y(u) + k_p Z(u) \tag{15}$$

Hence, for a fixed proportional gain $k_p = \tilde{k}_p$, there is a finite number of squared frequencies $\tilde{u}_i$, $i = 1, 2, \ldots, \tilde{n}$ that satisfy the following polynomial equation

$$F\left(\tilde{u}_i; \tilde{k}_p\right) = 0, i = 1, 2, \ldots, \tilde{n} \tag{16}$$

In fact, $\tilde{u}_i$ are the positive real roots of the polynomial $F\left(u; k_p\right)$. In the sequel, these $\tilde{u}_i$ are referred to as singular frequencies. For a singular frequency $\tilde{u}$, (13a) defines a straight line in the (k_i, k_d) plane. The following theorem characterizes the stability boundaries of the D-partition of the (k_i, k_d) plane.

Theorem 1: Given a characteristic polynomial $p(s; \mathbf{k})$ in (4), the set of stability boundaries of the D-partition of the (k_i, k_d) plane corresponding to a fixed $k_p = \tilde{k}_p$ consists of the following types of straight lines:

$$L_0 : k_i = 0 \tag{17a}$$

$$L_\infty : k_d = -\frac{b_m}{a_n}, \quad \text{if } m = n-1 \tag{17b}$$

$$L_l : k_i = \tilde{u}_l k_d + \frac{X(\tilde{u}_l)}{Z(\tilde{u}_l)}, \quad l = 1, 2, \ldots, \tilde{n} \tag{17c}$$

where $\tilde{u}_l, l = 1, 2, \ldots, \tilde{n}$ are the positive real roots of the polynomial (15) for $k_p = \tilde{k}_p$.

Theorem 1 is a slight modification of the result given by Söylemez et al. [29], and its proof follows directly from the derivations of (11)-(15). Here, it is noted that boundary lines L_0 and L_∞ (if they exist) are independent of the proportional gain parameter k_p whereas the line L_l depends implicitly on the k_p parameter. It should also be noted that the finite number of boundary lines defined by (17) divides the (k_i, k_d) plane into a finite number of non-overlapped convex polygons. This geometric property was first demonstrated by Ho et al. [25] using the Hermite-Biehler theorem and the linear programming technique.

Having characterized the *D*-partition stability regions in the two-dimensional (k_i, k_d) plane, we now proceed to provide a geometric or topological characterization of the *D*-partition of the three-dimensional parameter space $\mathbb{K}$. In fact, we are going to identify the critical points on the k_p axis for which a change in the topology of the *D*-partition of the (k_p, k_i, k_d) parameter space can occur only when the k_p parameter crosses a critical-k_p point.

Theorem 2: The topology of the *D*-partition of the (k_p, k_i, k_d) space can change only when the k_p parameter crosses a critical point that satisfies one of the following conditions:

(i) Two distinct singular lines L_i and L_k coincide.

(ii) One singular line L_i and border lines L_0 and L_∞ intersect at a single point.

(iii) Two distinct singular lines L_{i_i} and L_k intersect the border line L_0 at a common point.

(iv) Two distinct singular lines L_i and L_k intersect the border line L_∞ at a common point.

(v) Three distinct singular lines L_i, L_k and L_l intersect at a single point.

(vi) Value of the k_p function $f(u)$ at $u = 0$.

(vii)The bounded limit value of the k_p function as u approaches to ∞.

Before presenting a proof of this theorem, we first consider the issue of computing the aforementioned critical k_p points. To facilitate later explanations and references, we refer the critical k_p points that satisfy the conditions numbered (i)-(v) as types 1-5 critical k_p points, while conditions (vi) and (vii) are type-0 and type-∞ critical k_p points, respectively.

- Type-1 critical k_p points:

As shown in Fig. 2 (in Section IV), when the value of the k_p function $f(u)$ tends toward one of its local minima or maxima, two adjacent singular frequencies tend to move together. Consequenctly, the two corresponding singular lines tend to overlap. From such an obvious argument, we know that type-1 critical k_p points occur at those singular frequencies for which the k_p function $f(u)$ has local extrema. The necessary condition for the existence of the local extrema of the function $f(u)$ is given by

$$f'(u) = \frac{df(u)}{du} = 0 \tag{18}$$

Let the singular frequencies that satisfy the above condition be denoted by $\tilde{u}_l^1, l = 1, 2, \ldots, n_1$. From (15), we know that these singular frequencies are exactly the positive real roots of the polynomial:

$$V(u) = Y'(u) Z(u) - Y(u) Z'(u) \tag{19}$$

Hence, type-1 critical k_p points are evaluated as:

$$\tilde{k}_{p,l}^1 = -\frac{Y\left(\tilde{u}_l^1\right)}{Z\left(\tilde{u}_l^1\right)}, l = 1, 2, \ldots, n_1 \tag{20}$$

- Type-2 critical k_p points:

Suppose that border lines L_0 and L_∞ exist. Hence, the integral and derivative gains k_i and k_d corresponding to these lines are specified by (17a) and (17b), respectively. When a singular line L in the (k_i, k_d) plane passes through the point $(k_i^0, k_d^\infty) = (0, -a_n/b_{n-1})$, the intersection point of the border lines L_0 and L_∞, the corresponding singular frequency $\tilde{u}$ must satisfy the condition:

$$(k_i^0 - k_d^\infty \tilde{u}) Z(\tilde{u}) - X(\tilde{u}) = 0 \tag{21}$$

which is obtained from (13a). It can be seen that for a given k_i and k_d the above equation is a polynomial in the variable $\tilde{u}$. Let the positive real roots of the polynomial (21) be denoted by $\tilde{u}_l^2, l = 1, 2, \ldots, n_2$, the type-2 critical k_p points are then evaluated as:

$$\tilde{k}_{p,l}^2 = f\left(\tilde{u}_l^2\right) \tag{22}$$

- Type-3 critical k_p points:

Let L_1 and L_2 be singular lines corresponding to two distinct singular frequencies $\tilde{u}_1$ and $\tilde{u}_2$, respectively. Then, the three lines L_1, L_2 and L_0 intersect at a single point if the following conditions hold.

$$\begin{aligned} &\left(k_i^0 - k_d \tilde{u}_l\right) Z(\tilde{u}_l) - X(\tilde{u}_l) = 0, l = 1, 2 \\ &k_p Z(\tilde{u}_l) - X(\tilde{u}_l) = 0, l = 1, 2 \end{aligned} \tag{23}$$

The above four equations allow one to obtain four unknowns $\tilde{u}_1$, $\tilde{u}_2$, k_p, and k_d. Since the solutions to (23) are not necessarily unique, we denote the solution set as

$$\left(\tilde{k}_{p,l}^3, \tilde{k}_{d,l}^3, \tilde{u}_{1,l}^3, \tilde{u}_{2,l}^3\right), l = 1, 2, \ldots, n_3 \tag{24}$$

The k_p values $\tilde{k}_{p,l}^3, l = 1, 2, \ldots, n_3$ appearing in the above solution set are referred to as type-3 critical k_p points.

- Type-4 critical k_p points:

Suppose that the border line L_∞ exists, i.e. $m = n - 1$. Let L_1 and L_2 be singular lines corresponding to two distinct singular frequencies $\tilde{u}_1$ and $\tilde{u}_2$, respectively. Then the three lines L_1, L_2 and L_∞ intersect at a single point if the four conditions hold:

$$\begin{aligned} &\left(k_i - k_d^\infty \tilde{u}_l\right) Z(\tilde{u}_l) - X(\tilde{u}_l) = 0, l = 1, 2 \\ &k_p Z(\tilde{u}_l) - X(\tilde{u}_l) = 0, l = 1, 2 \end{aligned} \tag{25}$$

The above four polynomial equations allow one to find the four unknowns $\tilde{u}_1$, $\tilde{u}_2$, k_p, and k_i. As before, let the solution sets of (25) be denoted by

$$\left(\tilde{k}_{p,l}^4, \tilde{k}_{d,l}^4, \tilde{u}_{1,l}^4, \tilde{u}_{2,l}^4\right), \quad l = 1, 2, \ldots, n_4 \tag{26}$$

In the plane of $k_p = \tilde{k}_{p,l}^4$, the singular lines L_1 and L_2, which correspond to the singular frequencies $\tilde{u}_{1,l}^4$ and $\tilde{u}_{2,l}^4$, respectively, and the border line L_∞ intersect at the point in three-dimensional gain space, the point $(k_i, k_d) = (\tilde{k}_{i,k}^4, \tilde{k}_d^\infty)$. In the sequel, the k_p values $\tilde{k}_{p,l}^4, l = 1, 2, \ldots, n_4$, are referred to type-4 critical k_p points.

- Type-5 critical k_p points:

To determine the values of k_p for which the singular lines associated with three distinct singular frequencies intersect at a single point in the associated (k_i, k_d) plane, we set the equations.

$$\begin{aligned} &(k_i - k_d \tilde{u}_l) Z(\tilde{u}_l) - X(\tilde{u}_l) = 0, \\ &k_p Z(\tilde{u}_l) - X(\tilde{u}_l) = 0, l = 1, 2, 3 \end{aligned} \tag{27}$$

We solve this set of six simultaneous polynomial equations for the six unknowns to obtain the solution set

$$\left(\tilde{k}_{p,l}^5, \tilde{k}_{i,l}^5, \tilde{k}_{d,l}^5, \tilde{u}_{1,l}^5, \tilde{u}_{2,l}^5, \tilde{u}_{3,l}^5\right), l = 1, 2, \ldots, n_5 \tag{28}$$

The k_p values $\tilde{k}_{p,l}^5$ shown above are the type-5 critical k_p points.

- Type-0 critical k_p point:

The unique value of k_p function $f(u)$ evaluated at the zero singular frequency $u = 0$ is referred to as the type-0 critical k_p point and is denoted by

$$\tilde{k}_p^0 = f(0) < \infty \tag{29}$$

- Type-∞ critical k_p points:

Depending on the relative degrees of polynomials $A(s)$ and $B(s)$ the k_p function $f(u)$ may approach a finite value as the singular frequency u tends to ∞. In this case, the corresponding limit

$$\tilde{k}_p^\infty = \lim_{u\to\infty} f(u) \tag{30}$$

is referred to as the type-∞ critical point.

It should be mentioned that in [29] type-0 and type-1 critical k_p points were used to determine the stabilizing k_p-intervals. In this text, the presentation of type-3 and type-4

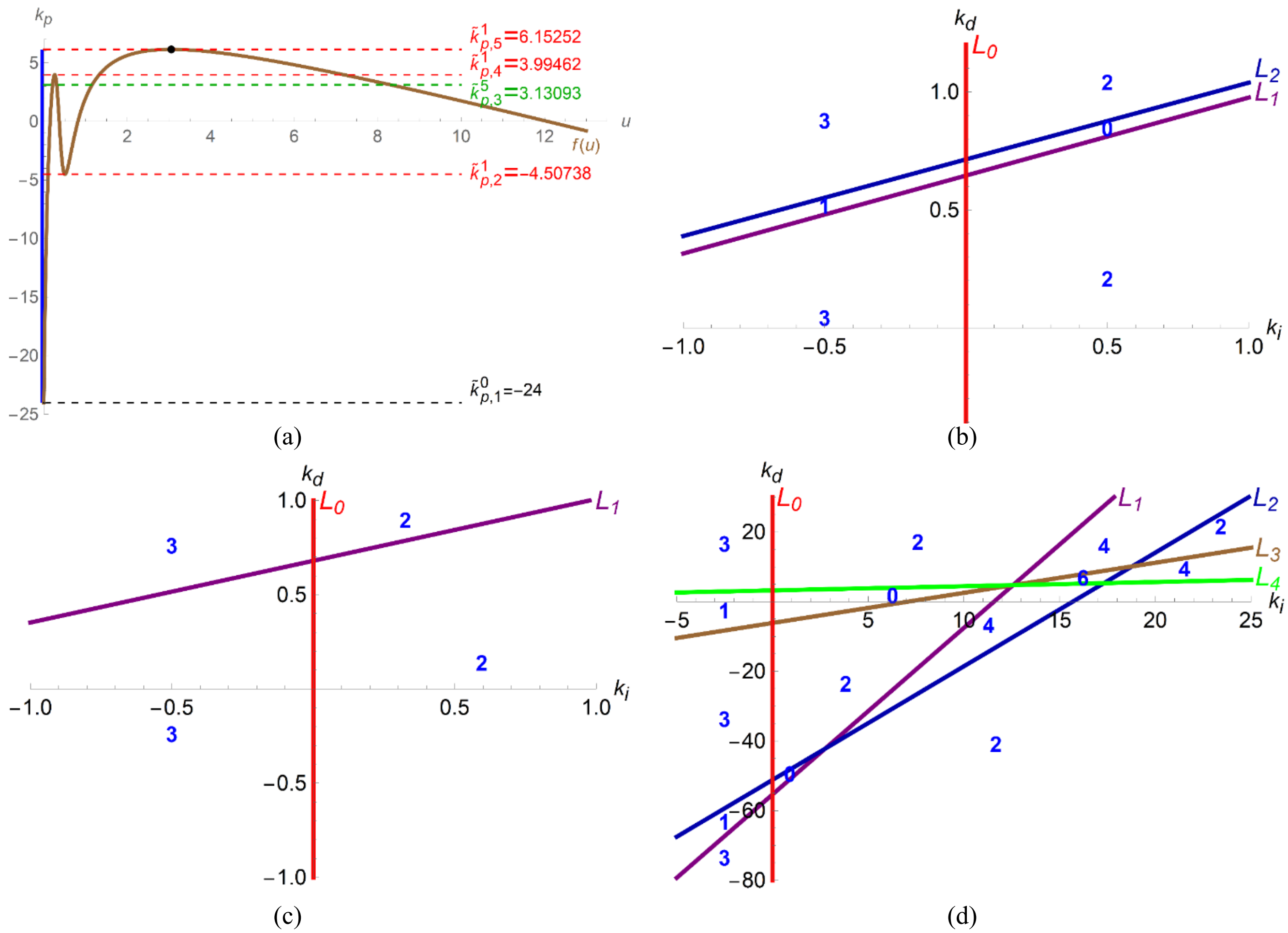

FIGURE 2. **(a). The plot of k_p function $f(u)$ vs u for Example 1. (b). The D-partition of the (k_i, k_d) plane for $k_p = \tilde{k}^1_{p,5} - 0.0002 = 6.1523$ in Example 1. (c). The D-partition of the (k_i, k_d) plane for $k_p = \tilde{k}^1_{p,5}$ in Example 1. (d). The D-partition of the (k_i, k_d) plane corresponding to the type-5 critical $k_p = \tilde{k}^5_{p,3} = 3.13093$ for Example 1.**

critical k_p points was inspired by [41]. Nevertheless, type-2, type-5, and type-∞ critical k_p points are identified for the first time. In other words, for linear continuous time-invariant systems, types 2-5 and type-∞ critical k_p points in the text are all newly presented.

Having identified the above seven types of possible critical points, we provide the following simple proof of Theorem 2. The proof is based on the property of the root-continuity argument [62], [63] and a simple geometrical interpretation of the deformation of plane polygons formed by a set of straight lines.

Proof of Theorem 2: As indicated in Theorem 1 the D-partition stability domains on each (k_i, k_d) plane of the three-dimensional PID gain space $\mathbb{K}$ are non-overlapped convex polygons that are formed by a set of singular lines together with the border lines L_0 and L_∞. The border lines L_0 and L_∞ are independent of the proportional gain parameter k_p whereas the singular lines are functions of singular frequencies, which in turn depend on parameter k_p. It is well known that the roots of a polynomial are continuous functions of its coefficients. As shown in (16), the singular frequencies $\tilde{u}_k$ are the roots of the polynomial $F(\tilde{u}; k_p)$ and parameter k_p enters the coefficients of the polynomial $F(\tilde{u}; k_p)$ in a linear manner. Moreover, the singular lines are continuous functions of k_p, that is, their slopes and axis intercept points vary continuously with respect to the continuous change in k_p. Consequently, the vertices of each stability polygons are also continuous functions of the proportional gain k_p. This fact implies that the topology or geometric structure of the D-partition stability polygons in the (k_i, k_d) plane can change only as the number of vertices of the stability polygons change when the parameter k_p is varied continuously. Indeed, when k_p moves continuously across a type-1 critical k_p point, the two singular lines coincide. In addition, when three D-partition boundary lines intersect at a single point, at least one stability triangle region disappears. Moreover, as k_p parameter passes through the type-0 or type-∞ (if any) critical k_p point, the number of singular lines can change, which in turn causes the topology of D-partition of the (k_i, k_d) plane to change. The proof is now completed based on the above arguments.

To construct the set of all stabilizing PID controllers, it is necessary to determine exactly and exhaustively the stabilizing k_p intervals within which each k_p corresponds to at least one stable region in the (k_i, k_d) plane. The following theorem serves as a means to identify the stabilizing k_p intervals from all critical k_p points.

Theorem 3: Let $\tilde{k}_{p,l}, l = 1, 2, \ldots, n_c$ denote all distinct critical k_p points arranged in ascending order, i.e. $\tilde{k}_{p,l} < \tilde{k}_{p,l+1}$. If for an arbitrary $k_p \in (\tilde{k}_{p,l}, \tilde{k}_{p,l+1}) := \mathbf{k}_{p,l}$ a stable polygon in the corresponding (k_i, k_d) plane exists, then there exists stable polygon(s) in the corresponding (k_i, k_d) plane for each $k_p \in \mathbf{k}_{p,l}$. Contrarily, if for a given k_p there is no any stable polygon in the correspondin g(k_i, k_d) plane then there has no k_p in the interval $\mathbf{k}_{p,l}$ to which the corresponding (k_i, k_d) plane has stable polygon.

Proof of Theorem 3: From (15), the singular frequencies u are the positive real roots of the k_p-parametrized polynomial $F(u; k_p)$. Hence, by the implicit function theorem we know that the root function $u(k_p)$ is continuous with respect to k_p everywhere except at the type-1 critical k_p points. According to the notion of critical k_p points, the topology of the D-partition of the (k_i, k_d) plane can change only when k_p moves across any of the k_p critical points. Consequently, the topology of the D-partition of the (k_i, k_d) plane remains invariant as k_p moves along the interval $\mathbf{k}_{p,l}$ which is formed by two adjacent critical k_p points. Hence, the existence or non-existence of stable region(s) in the (k_i, k_d) plane remains unchanged when the proportional gain k_p is varied within the interval $\mathbf{k}_{p,l}$ This completes the proof.

Before leaving this section, it is remarked that besides computing critical k_p values, all other computations involved in the construction of stabilizing PID set are essentially trivial. For a given plant, all the critical k_p values can be obtained by finding the real solutions of the four algebraic polynomial systems in (21), (23), (25), and (27), which respectively have one, two, four, and six unknowns. As commands or computer codes for computing all the real roots of polynomial systems have now become a quite standard feature of many commercially available mathematical software packages (e.g., Mathematica, Maple, and Matlab), determining all critical k_p values for a given plant can be easily accomplished.

IV. ILLUSTRATIVE EXAMPLES

To demonstrate the existence of seven types of critical k_p points and the construction of all stabilizing PID controllers, we provide five examples in this section. In the sequel, the blue figure labeled at the center of each polygon of the D-partition of (k_i, k_d) plane represents the number of unstable roots of the associated PID-controlled closed-loop. The numerical results and graphic drawings presented in this section were obtained using Wolfram Mathematica software [61] with double-precision computations. In the following five examples, the computer times spent to calculate the critical k_p values are 12, 12, 4, 2, and 2 seconds, respectively, on a PC equipped with Intel(R) i9-2.4GHz CPU.

Example 1: Consider the plant [29]:

$$G_{p,1}(s) = \frac{-4s^4 - 7s^3 - 2s + 1}{s^6 + 11s^5 + s^4 + 95s^3 + 109s^2 + 74s + 24}$$

The polynomials $X(u)$, $Y(u)$ and $Z(u)$ defined by (14) are evaluated to be

$$\begin{aligned} X(u) &= -122u + 481u^2 - 792u^3 + 229u^4 + 4u^5, \\ Y(u) &= 24 - 275u + 730u^2 - 579u^3 + 31u^4 + u^5, \\ Z(u) &= 1 + 4u - 30u^2 + 49u^3 + u^4. \end{aligned}$$

Following the procedure given in Section III, we obtain the following critical k_p values and associated singular frequencies.

$$\begin{aligned} \left(\tilde{k}^0_{p,1}, \tilde{u}^0\right) &= (-24, 0), \\ \left(\tilde{k}^0_{p,2}, \tilde{u}^1_1\right) &= (-4.50738, 0.506408), \\ \left(\tilde{k}^5_{p,3}, \tilde{k}^5_{i,3}, \tilde{k}^5_{d,3}, \tilde{u}^5_1, \tilde{u}^5_2, \tilde{u}^5_3\right) &= (3.1309, 12.5617, 4.74246, \\ &\qquad 0.208996, 1.156356, 8.30647), \\ \left(\tilde{k}^1_{p,4}, \tilde{u}^1_2\right) &= (3.99, 0.258438), \\ \left(\tilde{k}^1_{p,5}, \tilde{u}^1_3\right) &= (6.15252, 3.05170). \end{aligned}$$

Here the superscripted number stands for the type of critical k_p value.

The plot k_p function $f(u)$ is shown in Fig. 2(a), in which all the critical k_p values are also depicted. In this plot, the blue segment on the k_p-axis represents the stabilizing k_p interval. Referring to Fig. 2(a), the coordinate of the black-dotted point on the curve of $f(u)$ is $\left(u, k_p\right) = \left(\tilde{u}^1_3, \tilde{k}^1_{p,5}\right) = (3.0517, 6.1525)$. It can be seen from this figure that the horizontal line of constant k_p with its value slightly less than the critical k_p value $\tilde{k}^1_{p,5}$, will intersect with the k_p function $f(u)$ at two points. For instance, the horizontal line of $k_p = \tilde{k}^1_{p,5} - \varepsilon = 6.1523$, $\varepsilon = 0.0002$, and the two intersection points are at $u_1 = 3.0260$ and $u_2 = 3.0776$, which are very close to the singular frequency $u = \tilde{u}^1_3$. As shown in Fig. 2(b), the boundary lines L_1 and L_2 corresponding to these two singular frequencies on plane $k_p = 6.1523$ are almost parallel to each other because their slopes are $1/u_1$ and $1/u_2$ respectively. As $k_p \uparrow \tilde{k}^1_{p,5}$, the corresponding singular frequencies $u_1 \uparrow \tilde{u}^1_3$ and $u_2 \downarrow \tilde{u}^1_3$. This indicates that the two boundary lines L_1 and L_2 coincide as $k_p \uparrow \tilde{k}^1_{p,5}$, as shown in Fig. 1(c).

The D-partition of the (k_i, k_d) plane associated with the type-5 critical k_p point, $\tilde{k}^5_{p,3}$, was constructed as shown in Fig. 2(d). It can be observed that three singular lines intersect at a single point $(k_i, k_d) = (\tilde{k}^5_{i,3}, \tilde{k}^5_{d,3})$.

Example 2: For the plant's transfer function

$$G_{p,2}(s) = \frac{-s^4 - 5s^3 + 8s^2 - s - 1}{s^5 + 3s^4 + 29s^3 + 15s^2 - 3s + 1}$$

all its critical k_p points and the corresponding singular frequencies are as follows:

$$\left(\tilde{k}_{p,1}^{\infty}, \tilde{u}^{\infty}\right) = (-2, \infty),$$
$$\left(\tilde{k}_{p,2}^{1}, \tilde{u}_1^{1}\right) = (-0.77850, 0.28893),$$
$$\left(\tilde{k}_{p,3}^{3}, \tilde{k}_{i,3}^{3}, \tilde{k}_{d,3}^{3}, \tilde{u}_1^{3}, \tilde{u}_2^{3}\right) = (-0.059346, 0, -3.017424, 0.87070),$$
$$\left(\tilde{k}_{p,4}^{0}, \tilde{u}^{0}\right) = (1, 0),$$
$$\left(\tilde{k}_{p,5}^{1}, \tilde{u}_2^{1}\right) = (2.17883, 7.94694),$$

A plot k_p function, $f(u)$, is shown in Fig. 3(a). Since the relative degree of the denominator and numerator polynomials of $G_{p,2}(s)$ is one, both border lines L_0 and L_∞ exist, i.e., $k_i = 0$ and $k_d = 1$. Moreover, a type-∞ critical k_p point exists. The data above also indicate that there is a type-3 critical k_p point at which two boundary lines and the border line L_0 intersect at a single point $(k_i, k_d) = \left(\tilde{k}_{i,3}^{3}, \tilde{k}_{d,3}^{3}\right) = (0, -3.17424)$ on the (k_i, k_d) plane. This can be verified by the D-partition of the (k_i, k_d) plane with $k_p = \tilde{k}_{p,3}^{3}$ shown in Fig. 3(b).

Example 3: Consider the six-order plant

$$G_{p,3}(s) = (1-s)\, G_{p,1}(s) = \frac{s^5 + 6s^4 - 7s^3 + 2s^2 - 3s + 1}{s^6 + 11s^5 + s^4 + 95s^3 + 109s^2 + 74s + 24}$$

where $G_{p,1}(s)$ denotes the plant shown in **Example 1**. All poles and zeros of $G_{p,3}(s)$ are exactly the same as those of $G_{p,1}(s)$ except that it has an additional non-minimum-phase zero at $s = 1$. The k_p function $f(u)$ for this plane is shown in Fig. 4(a). Clearly, border lines L_0 and L_∞ exist, i.e., $k_i = 0$ and $k_d = -1$. Subsequently, using the formulas given in (18)-(30), we obtain six critical k_p points for the D-partition of the PID parameter space. The values and types of critical k_p points and the associated singular frequencies are as follows:

$$\left(\tilde{k}_{p,1}^{0}, \tilde{u}^{0}\right) = (-24, 0),$$
$$\left(\tilde{k}_{p,2}^{1}, \tilde{u}_1^{1}\right) = (-5.01468, 315.111),$$
$$\left(\tilde{k}_{p,3}^{\infty}, \tilde{u}^{\infty}\right) = (-5, \infty),$$
$$\left(\tilde{k}_{p,4}^{2}, \tilde{k}_{i,4}^{2}, \tilde{k}_{d,4}^{2}, \tilde{u}^{2}\right) = (4.63153, 0, -1, 1.20748),$$
$$\left(\tilde{k}_{p,5}^{4}, \tilde{k}_{i,5}^{4}, \tilde{k}_{d,5}^{4}, \tilde{u}_1^{4}, \tilde{u}_2^{4}\right) = (5.34403, 7.31838, -1, 0.12294, 0.65058),$$
$$\left(\tilde{k}_{p,6}^{1}, \tilde{u}_2^{1}\right) = (14.4637, 0.29311).$$

As indicated in the above data set or in Fig. 4(a), there are five different types of critical k_p points. Fig. 4(b) shows the D-partition of the (k_i, k_d) plane with the type-2 critical k_p point, $k_p = \tilde{k}_{p,4}^{2}$. It can be observed from this figure that the singular line L_2 associated with $u = \tilde{u}^2$ passes through the point $(k_i, k_d) = (0, -1)$ which is the intersection point of the border lines L_0 and L_∞. For the type-4 critical k_p point, $k_p = \tilde{k}_{p,5}^{4}$, the D-partition of the corresponding (k_i, k_d) plane is depicted in Fig. 4(c). As can be observed, the three boundary lines L_∞, $L_{\tilde{u}_1^4}$ and $L_{\tilde{u}_2^4}$ intersect at point $(k_i, k_d) = \left(\tilde{k}_{i,5}^{4}, -1\right)$.

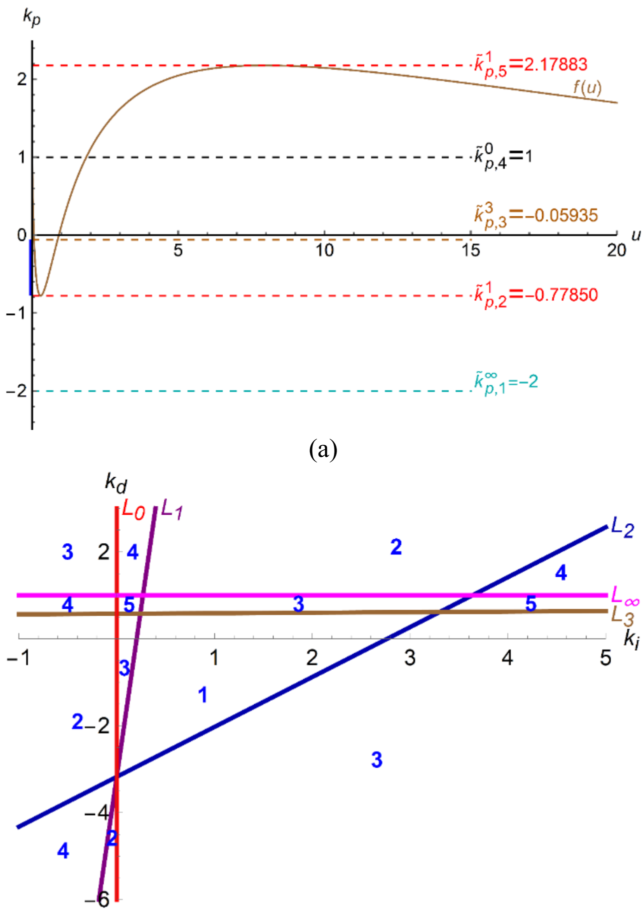

FIGURE 3. **(a). The plot of k_p function $f(u)$ vs u for Example 2. (b). The D-partition of the (k_i, k_d) plane corresponding to $k_p = \tilde{k}_{p,3}^{3}$ for Example 2.**

Example 4: Consider the plant

$$G_{p,4}(s) = \frac{s^3 + 3s^2 + 9}{s^4 + 2s^3 + 3s^2 + 7s + 14}$$

The k_p function, $f(u)$, is plotted in Fig. 5(a). It can be seen from this figure that there are two disjoint stabilizing k_p intervals, i.e., $(\tilde{k}_{p,1}^{1}, \tilde{k}_{p,3}^{1})$ and $(\tilde{k}_{p,4}^{1}, \tilde{k}_{p,6}^{1})$ The entire set of stabilizing PID controller parameters is shown in Fig. 5(b). In addition, seven critical k_p points are identified. The seven critical k_p points shown in this figure and their associated singular frequencies are listed below:

$$\left(\tilde{k}_{p,1}^{1}, \tilde{u}_1^{1}\right) = (-1.87078, 1.36615),$$
$$\left(\tilde{k}_{p,2}^{2}, \tilde{u}_1^{2}\right) = (-1.73465, 0.73135),$$
$$\left(\tilde{k}_{p,3}^{0}, \tilde{u}^{0}\right) = (-1.55555, 0),$$
$$\left(\tilde{k}_{p,4}^{1}, \tilde{u}_2^{1}\right) = (0.315687, 8.62419),$$

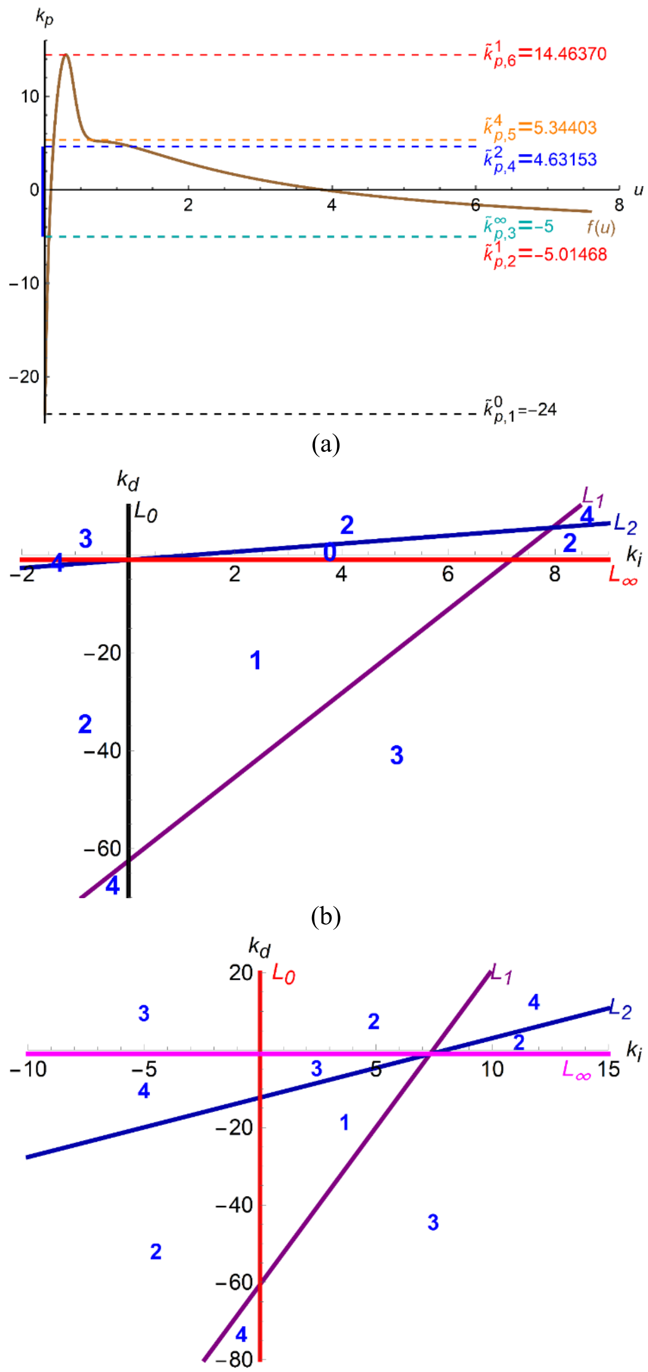

(a)

(b)

(c)

FIGURE 4. (a). The plot of k_p function $f(u)$ vs u for Example 3. (b). The D-partition of the (k_i, k_d) plane corresponding to the type-2 critical $k_p = \tilde{k}^2_{p,4}$ (c). The D-partition of the (k_i, k_d) plane corresponding to the type-4 critical $k_p = \tilde{k}^4_{p,5}$.

$$\left(\tilde{k}^2_{p,5}, \tilde{u}^2_2\right) = (0.51243, 4.102)\,,$$
$$\left(\tilde{k}^1_{p,6}, \tilde{u}^1_3\right) = (0.533262, 3.70234)\,,$$
$$\left(\tilde{k}^\infty_{p,7}, \tilde{u}^\infty\right) = (1, \infty)\,,$$

From the data set shown above, we see that there are two type-2 critical k_p points, i.e., $k_p = \tilde{k}^2_{p,2}$ and $k_p = \tilde{k}^2_{p,5}$. Hence, it can be verified that in the (k_i, k_d) plane associated with $k_p = \tilde{k}^2_{p,2}$ (resp. $k_p = \tilde{k}^2_{p,5}$), and boundary lines L_0, L_∞ and $L(u = \tilde{u}^2_1)$ (resp. $L(u = \tilde{u}^2_2)$) intersects at point $(k_i, k_d) = (0, 1)$.

To show the detail of constructing D-partition of the (k_i, k_d)-plane associated with the $\tilde{k}_p = -1.80272$, which is the mid-point of the stabilizing k_p-interval $[\tilde{k}^1_{p,1}, \tilde{k}^2_{p,2}]$. The positive real roots of the polynomial $F[u, \tilde{k}_p]$ are found to be $\tilde{u}_1 = 0.96975$ and $\tilde{u}_2 = 1.6447$. The four D-partition boundary lines are thus given by

$$L_0 : k_i = 0$$
$$L_\infty : k_d = -1$$
$$L_1 : k_i - 0.96975 k_d = 1.08406$$
$$L_2 : k_i - 0.96975 k_d = 2.70038$$

With these four lines the partition of the (k_i, k_d)-plane is shown in Figure 5(c). In this figure, the (k_i, k_d)-plane is divided into 11 non-overlapped polygons and each blue-colored figure signify the number of unstable roots of the corresponding characteristic polynomial with (k_i, k_d) controller parameters being taken from each stability domain while keeping $\tilde{k}_p = -1.80272$. The existence of stable polygon (0 unstable roots) with the vertices $(0, -1.11787)$, $(-1.23818, -2.39468)$, and $(0, -1.64185)$, confirms that $[\tilde{k}^1_{p,1}, \tilde{k}^2_{p,2}]$ belongs to the set of stabilizing k_p-intervals. The geometric center of the stable polygon is evaluated to be $(\tilde{k}_i, \tilde{k}_d) = (-0.412727, -1.71813)$. For the PID controller setting $(\tilde{k}_d, \tilde{k}_i, \tilde{k}_d)$, the closed-loop characteristic polynomial is given by

$$P(s) = -3.71454 - 2.22446s - 9.70139s^2 - 2.82088s^3 - 4.95712s^4 - 0.718134s^5$$

which has the following five roots:

$$-6.60969,$$
$$-0.108054 \pm 0.733117\,\mathrm{i},$$
$$-0.0384902 \pm 1.19315\,\mathrm{i}$$

All the real parts of these roots are negative, the PID-controlled system is thus stable.

Example 5: Consider the control of the discrete-time system

$$G_{p,5}(z) = \frac{100sz^3 + 8z^2 + 3z + 11}{100z^5 + 2z^4 + 5sz^3 - 41z^2 + 52z + 70}$$

using a discrete-time PID controller of the form

$$G_c(z) = K_p + \frac{K_i}{(1 - z^{-1})} + K_d(1 - z^{-1})$$

The application of bilinear transform

$$z = \frac{s+1}{s-1}$$

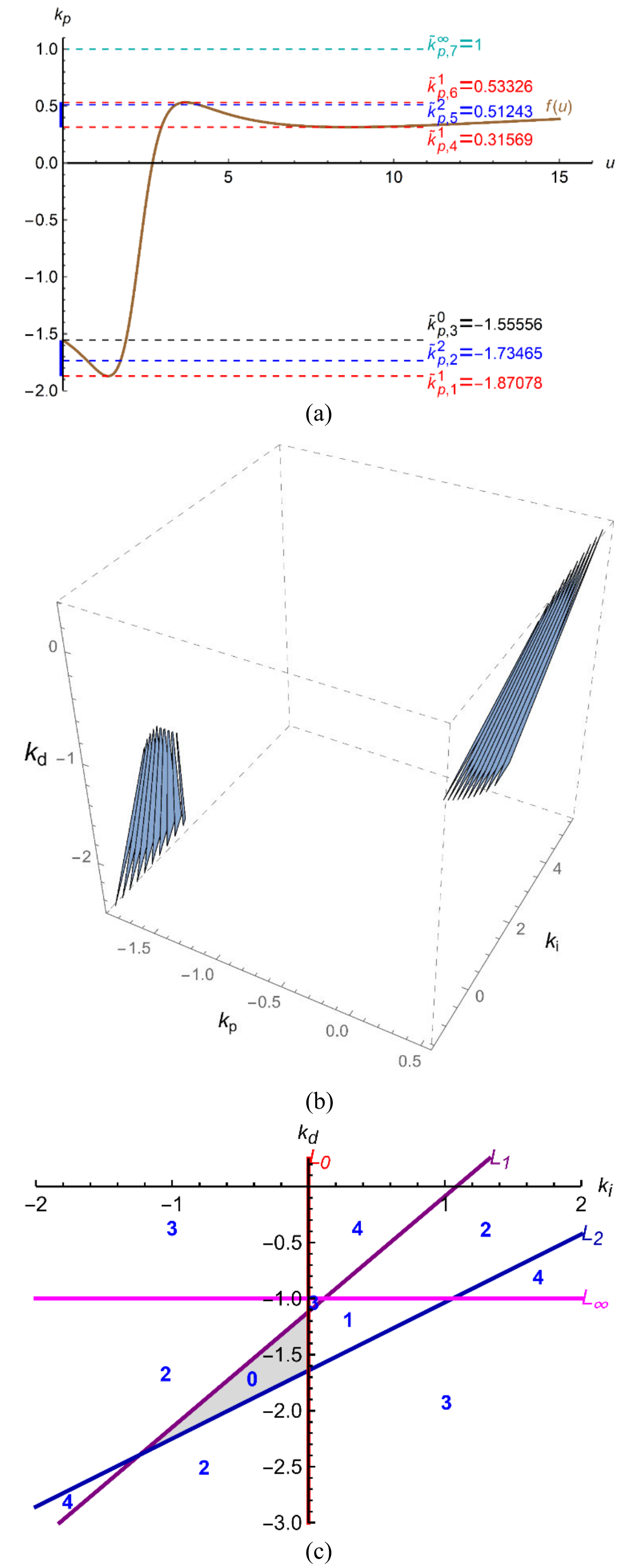

FIGURE 5. (a). The plot of k_p function $f(u)$ for Example 4. (b). The entire set of stabilizing PID controller parameters for Example 4, in which the stabilizing k_p intervals are $\left(\tilde{k}^1_{p,1}, \tilde{k}^1_{p,3}\right) = (-1.87078, -1.55555$ and $\left(\tilde{k}^1_{p,4}, \tilde{k}^1_{p,6}\right) = (0.315687, 0.533262)$. (c). The D-partition of the (k_i, k_d)-plane associated with the k_p value $k_{p=} -1.80272$ for Example 4.

leads to the following equivalent characteristic polynomial

$$p\left(s; k_p, k_i, k_d\right) = A\left(s\right) + \left(k_i + k_p s + k_d s^2\right) B(s)$$

where

$$A\left(s\right) = 63 + 389s + 480s^2 + 1094s^3 + 963s^4 + 117s^5 + 94s^6$$
$$B\left(s\right) = 45 + 74s - 150s^2 - 44s^3 + 17s^4 + 58s^5$$

Hence, the RRB ∂D_0 and IRB ∂D_∞ of the D-partition of the (k_p, k_i, k_d) parameter space are given by

$$\partial D_0 : k_i = -A(0)/B(0) = -1.4$$
$$\partial D_\infty : k_d = 0$$

For the characteristic polynomial $p\left(s; k_p, k_i, k_d\right)$, the k_p function, $f(u)$, is plotted in Fig. 6(a). All critical k_p points and their corresponding singular frequencies are obtained as follows:

$$\left(\tilde{k}^0_{p,1}, \tilde{u}^0\right) = (-6.34222, 0)\,,$$
$$\left(\tilde{k}^\infty_{p,2}, \tilde{u}^\infty\right) = (-1.62069, \infty)\,,$$
$$\left(\tilde{k}^2_{p,3}, \tilde{k}^2_{i,3}, \tilde{k}^2_{d,3}, \tilde{u}^2\right) = (-1.48947, -1.4, 0, 131.441)\,,$$
$$\left(\tilde{k}^4_{p,4}, \tilde{k}^4_{i,4}, \tilde{k}^4_{d,4}, \tilde{u}^4_1, \tilde{u}^4_2\right) = (0.050947, -0.09676, 0, 0.366004, 9.3496),$$
$$\left(\tilde{k}^1_{p,5}, \tilde{u}^1\right) = (3.0669, 1.56195)\,.$$

The stabilizing k_p interval is found to be $\left(\tilde{k}^\infty_{p,2}, \tilde{k}^4_{p,4}\right)$. To verify that the type-∞ critical k_p point $\tilde{k}^\infty_{p,2}$ is the endpoint of the stabilizing interval, we construct the D-partitions of (k_i, k_d) planes with $k_p = -3.98146$ and $k_p = -1.55508$, respectively, which are the middle points of the intervals $\left(\tilde{k}^0_{p,1}, \tilde{k}^\infty_{p,2}\right)$ and $\left(\tilde{k}^\infty_{p,2}, \tilde{k}^2_{p,3}\right)$. For $k_p = -3.98146$, the D-partition of the associated $k_p = -3.98146$ plane is shown in Fig. 6(b). As shown in the figure, none of the stability regions are stable. However, for $k_p = -1.55508$, we take $\{k_i, k_d\} = \{-0.90614, 0.00107\}$, which is the center of the stable polygon, to form the characteristic polynomial

$$p\left(s; k_p, k_i, k_d\right) = 22.224 + 251.967s + 500.893s^2 1367.211s^3 + 1015.859s^4 + 37.9604s^5 + 3.82355s^6 + 0.0620s^7$$

It can be checked that the above polynomial is Hurwitz stable.

In Table 1, we summarize all the critical k_p points on the k_p-axis for the plants considered in this section. In this table, different types of k_p points are marked with different colors, and the stabilizing k_p intervals are shown in green line segments. It can be seen from the table that seven types of critical k_p points exist for the PID control of different plants. In addition, except for type-2 and type-5 critical k_p points, all the other five types of critical k_p]points may appear as one of the endpoints of a stabilizing k_p interval. In the literature,

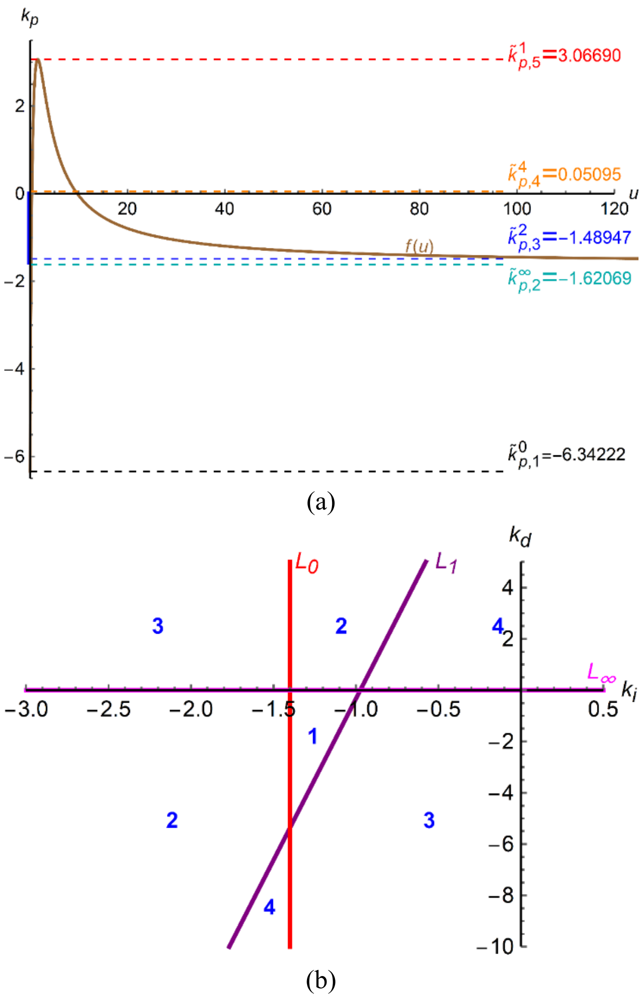

FIGURE 6. (a). The plot off k_p function $f(u)$ vs u for Example 5. (b). The D-partition of the $k_p = -3.98146$ plane in the PID parameter space.

TABLE 1. Critical points and types for plants in examples 1-5.

Plant	Critical k_p points and types
$G_{p,1}(s)$	Type → 0, 1, 5 1 1; $-\infty$ → $k_p \to \infty$; $\tilde{k}_{p,j}$, j → 1, 2, 3 4 5
$G_{p,2}(s)$	Type → ∞, 1, 3, 0, 1; $-\infty$ → $k_p \to \infty$; $\tilde{k}_{p,j}$, j → 1, 2, 3, 4, 5
$G_{p,3}(s)$	Type → 1, ∞ 0, 2 4, 1; $-\infty$ → $k_p \to \infty$; $\tilde{k}_{p,j}$, j → 1, 3 2, 4 5, 6
$G_{p,4}(s)$	Type → 1 2 0, 1 2 1, ∞; $-\infty$ → $k_p \to \infty$; $\tilde{k}_{p,j}$, j → 1 2 3, 4 5 6, 7
$G_{p,5}(s)$	Type → 0, ∞ 2, 4, 1; $-\infty$ → $k_p \to \infty$; $\tilde{k}_{p,j}$, j → 1, 2 3, 4, 5

only type-0 and type-1 critical k_p points have been used to determine the stabilizing k_p intervals, which can lead to an inexact PID stabilizing set. For example, by the criterion given in the existing literature, e.g., [29], only type-0 and type-1 critical k_p points $\tilde{k}^1_{p,2} = -0.77850, \tilde{k}^0_{p,4} = 1$, and $\tilde{k}^1_{p,5} = 2.17883$ would be identified. By sampling any k_p point from the interval $I_{4,5} = (\tilde{k}^0_{p,4}, \tilde{k}^1_{p,5})$, one can conclude that interval $I_{4,5}$ is not a stabilizing k_p -interval. However, the lack of type-3 critical $\tilde{k}^3_{p,3} = -0.059346$ would lead one to conclude that $I_{4,5} = (\tilde{k}^0_{p,2}, \tilde{k}^1_{p,4})$ is a stabilizing k_p-interval if a k_p point is sampled from the interval $I_{2,3} = (\tilde{k}^0_{p,2}, \tilde{k}^3_{p,3})$, or that $I_{4,5}$ is not a stabilizing k_p-interval if a k_p is sampled from the interval $I_{3,4} = (\tilde{k}^4_{p,3}, \tilde{k}^1_{p,4})$. However, the finding of type-3 critical $\tilde{k}^3_{p,3} = -0.059346$ allows one to conclude exactly that the interval $I_{2,3}$ is a stabilizing k_p-interval while the interval $I_{3,4}$ is not. An exact determination of stabilizing k_p-intervals will occur for Example 5 if only type-0 and type-1 critical k_p points are used without taking into account the existence of type-∞ and type-4 critical k_p points $\tilde{k}^\infty_{p,2} = -1.62069$ and $\tilde{k}^4_{p,4} = 0.050947$.

V. CONCLUSION

In this study, the problem of finding the entire set of stabilizing PID controllers for a linear time-invariant plant of arbitrary order has been fully solved. The successful resolution of the problem is based on using the D-partition technique and the unique feature of the stabilizing PID controller set that for a given proportional gain k_p, the D-partition boundaries in the (k_i, k_d) plane are all straight lines. By characterizing the topology change of the D-partition regions in the (k_i, k_d) plane with the respective proportional gain parameter k_p, we have presented the notion critical k_p points. More importantly, we have identified seven types of critical points and provided their computational formulas. Consequently, all stabilizing k_p-intervals can be determined exactly and exhaustively. Thus, the presented analytical characterization of the stabilizing PID controller set is complete and constructive. This new characterization can facilitate the construction of controller parameter domains that meet design specifications such as gain margin, phase margin, degree of stability and sensitivity. Therefore, it is believed that the presented results will enlarge the application of the D-partition technique to cases where the number of controller parameters is more than three.

REFERENCES

[1] K. J. Åström and T. Hägglund, *Advanced PID Control*. Research Triangle Park, NC, USA: The Instrumentation, Systems, and Automation Society, 2006.

[2] A. O'Dwyer, *Handbook of PI and PID Controller Tuning Rules*, 2nd ed. London, U.K.: Imperial College Press, 2006.

[3] I. D. Díaz-Rodríguez, H. Sangjin, and S. P. Bhattacharyya, *Analytical Design of PID Controllers*. Berlin, Germany: Springer, 2019.

[4] R. Vilanova and A. Visioli, *PID Control in the Third Millennium-Lessons Learned and New Approaches*. London, U.K.: Springer, 2012.

[5] R. P. Borase, D. K. Maghade, S. Y. Sondkar, and S. N. Pawar, "A review of PID control, tuning methods and applications," *Int. J. Dyn. Control*, vol. 9, no. 2, pp. 818–827, Jun. 2021.

[6] S. M. Hassan, R. Ibrahim, N. Saad, K. Bingi, and V. S. Asirvadam, *Hybrid PID Based Predictive Control Strategies for WirelessHART Networked Control Systems*. Cham, Switzerland: Springer, 2020.

[7] J. Alcaina, A. Cuenca, J. Salt, V. Casanova, and R. Pizá, "Delay-independent dual-rate PID controller for a packet-based networked control system," *Inf. Sci.*, vol. 484, pp. 27–43, May 2019.
[8] T. Shibata and T. Murakami, "Null space motion control by PID control considering passivity in redundant manipulator," *IEEE Trans. Ind. Informat.*, vol. 4, no. 4, pp. 261–270, Nov. 2008.
[9] I. Mahtout, F. Navas, V. Milanes, and F. Nashashibi, "Advances in Youla–Kucera parametrization: A review," *Annu. Rev. Control*, vol. 49, pp. 81–94, Jun. 2020.
[10] D. Youla, J. Bongiorno, and H. Jabr, "Modern wiener-hopf design of optimal controllers. Part I: The single-input-output case," *IEEE Trans. Autom. Control*, vol. AC-21, no. 1, pp. 3–13, Feb. 1976.
[11] B. Zhou and J. L. Speyer, "$\mathcal{H}_2$ control of SISO fractional order systems," *Syst. Control. Lett.*, vol. 132, no. 1, Oct. 2019, Art. no. 104511.
[12] F. A. Aliev and V. B. Larin, "Parametrization of sets of stabilizing controllers in mechanical systems," *Int. Appl. Mech.*, vol. 44, no. 6, pp. 599–618, Oct. 2008.
[13] E. Polak, "A modified Nyquist stability test for use in computer-aided design," *IEEE Trans. Autom. Control*, vol. AC-29, no. 1, pp. 91–93, Jan. 1984.
[14] L. Trybus and Z. Świder, "Root-locus design of PID controller for an unstable plant," in *Trends in Advanced Intelligent Control, Optimization and Automation*, W. Mitkowski, J. Kacprzyk, K. Oprzędkiewicz, and P. Skruch, Eds. Cham, Switzerland: Springer, 2017, pp. 14–20.
[15] B. S. Nesimioglu and M. T. Soylemez, "Calculation of all gains providing time-delay independent stability via root locus," in *Proc. Int. Conf. Control, Decis. Inf. Technol. (CoDIT)*, Metz, France, Nov. 2014, pp. 566–571.
[16] P. Tsiotras, "The relation between the 3-D Bode diagram and the root locus: Insights into the connection between these classical methods," *IEEE Contr. Syst. Mag.*, vol. 25, no. 1, pp. 88–96, Feb. 2005.
[17] B. A. Angélico, L. B. G. Campanhol, and S. A. O. da Silva, "Proportional–integral/proportional–integral-derivative tuning procedure of a single-phase shunt active power filter using Bode diagram," *IET Power Electron.*, vol. 7, no. 10, pp. 2647–2659, Oct. 2014.
[18] P. C. Byrne, J. Li, and M. R. Parker, "Nichols chart design software," in *Proc. IEEE Energy Inf. Technol. Southeast*, vol. 3. Columbia, SC, USA, Apr. 1989, pp. 1281–1283, doi: 10.1109/SECON.1989.132628.
[19] J. Wilkie, M. Johnson, and R. Katebi, "Analysis and simple design using the Nichols chart," in *Control Engineering*. London, U.K.: Red Globe Press, 2002, pp. 505–528, doi: 10.1007/978-1-4039-1457-6_17.
[20] B. Porter, *Stability Criteria for Linear Dynamical Systems*. New York, NY, USA: Academic, 1967.
[21] J. I. Neimark, "D-decomposition of the space of quasi-polynomials," *Amer. Math. Soc. Trans.*, vol. 2, pp. 95–131, Jan. 1973.
[22] E. N. Gryazina and B. T. Polyak, "Stability regions in the parameter space: D-decomposition revisited," *Automatica*, vol. 42, no. 1, pp. 13–26, Jan. 2006.
[23] M. N. Ali, M. Soliman, K. Mahmoud, J. M. Guerrero, M. Lehtonen, and M. M. F. Darwish, "Resilient design of robust multi-objectives PID controllers for automatic voltage regulators: D-decomposition approach," *IEEE Access*, vol. 9, pp. 106589–106605, 2021.
[24] N. Munro, "The systematic design of PID controllers using Nyquist stabiliy," in *Proc. Eur. Control Conf. (ECC)*, Porto, Portugal, Sep. 2001, pp. 528–533, doi: 10.23919/ecc.2001.7075961.
[25] M.-T. Ho, A. Datta, and S. P. Bhattacharyya, "A linear programming characterization of all stabilizing PID controllers," in *Proc. Amer. Control Conf.*, Albuquerque, NM, USA, 1997, pp. 3922–3928.
[26] M. Saeki, "Properties of stabilizing PID gain set in parameter space," *IEEE Trans. Autom. Control*, vol. 52, no. 9, pp. 1710–1715, Sep. 2007.
[27] J. Bu, A. Mesbahi, and M. Mesbahi, "On topological properties of the set of stabilizing feedback gains," *IEEE Trans. Autom. Control*, vol. 66, no. 2, pp. 730–744, Feb. 2021.
[28] D. Ma, S. Niculescu, L. Guo, and J. Chen, "Special issue on PID control in the information age: Theoretical advances and applications," *Int. J. Robust Nonlinear Control*, vol. 32, no. 18, pp. 9384–9388, Dec. 2022, doi: 10.1002/rnc.6410.
[29] M. T. Söylemez, N. Munro, and H. Baki, "Fast calculation of stabilizing PID controllers," *Automatica*, vol. 39, no. 1, pp. 121–126, Jan. 2003.
[30] M.-T. Ho, A. Datta, and S. P. Bhattachary, "Control system design using low order controllers: Constant gain, PI and PID," in *Proc. Amer. Control Conf.*, Albuquerque, NM, USA, 1997, pp. 571–578.
[31] J. Ackermann and D. Kaesbauer, "Stable polyhedra in parameter space," *Automatica*, vol. 39, no. 5, pp. 937–943, May 2003.
[32] B. N. Le, Q.-G. Wang, and T. H. Lee, "Development of D-decomposition method for computing stabilizing gain ranges for general delay systems," *J. Process Control*, vol. 25, pp. 94–104, Jan. 2015.
[33] L. H. Keel and S. P. Bhattacharyya, "A Bode plot characterization of all stabilizing controllers," *IEEE Trans. Autom. Control*, vol. 55, no. 11, pp. 2650–2654, Nov. 2010.
[34] N. Bajcinca, "Design of robust PID controllers using decoupling at singular frequencies," *Automatica*, vol. 42, no. 11, pp. 1943–1949, Nov. 2006.
[35] N. Tan, I. Kaya, C. Yeroglu, and D. P. Atherton, "Computation of stabilizing PI and PID controllers using the stability boundary locus," *Energy Convers. Manage.*, vol. 47, nos. 18–19, pp. 3045–3058, Nov. 2006.
[36] E. Almodaresi, M. Bozorg, and H. D. Taghirad, "Stability domains of the delay and PID coefficients for general time-delay systems," *Int. J. Control*, vol. 89, no. 4, pp. 783–792, Apr. 2016.
[37] I. D. Díaz-Rodríguez, S. Han, and S. P. Bhattacharyya, *Analytical Design of PID Controllers*. London, U.K.: Springer, 2019.
[38] X.-G. Li, S.-I. Niculescu, J.-X. Chen, and T. Chai, "Characterizing PID controllers for linear time-delay systems: A parameter-space approach," *IEEE Trans. Autom. Control*, vol. 66, no. 10, pp. 4499–4513, Oct. 2021.
[39] N. Tan and D. P. Atherton, "Design of stabilizing PI and PID controllers," *Int. J. Syst. Sci.*, vol. 37, no. 8, pp. 543–554, Jun. 2006.
[40] T.-Y. Guo, L.-S. Lu, S.-Y. Lin, and C. Hwang, "Design of maximum-stability PID controllers for LTI systems based on a stabilizing-set construction method," *J. Taiwan Inst. Chem. Eng.*, vol. 135, Jun. 2022, Art. no. 104366.
[41] T. Guo, C. Hwang, and L. Lu, "Design of discrete PID controllers for maximizing stability margins," *Asian J. Control*, vol. 25, no. 2, pp. 824–839, Mar. 2023.
[42] R. Frazer and W. Duncan, "On the criteria for the stability of small motions," *Proc. Roy. Soc. London A, Containing Papers Math. Phys. Character*, vol. 124, no. 795, pp. 642–654, 1929.
[43] R. Lanzkron and T. Higgins, "D-decomposition analysis of automatic control systems," *IRE Trans. Autom. Control*, vol. 4, no. 3, pp. 150–171, Dec. 1959.
[44] E. Polak, "A note on D-decomposition theory," *IEEE Trans. Autom. Control*, vol. AC-9, no. 1, pp. 107–109, Jan. 1964.
[45] E. N. Gryazina, "The D-decomposition theory," *Autom. Remote Control*, vol. 65, no. 12, pp. 1872–1884, 2004.
[46] D. D. Siljak, "Analysis and synthesis of feedback control systems in the parameter plane I-linear continuous systems," *IEEE Trans. Appl. Ind.*, vol. AI-83, no. 75, pp. 449–458, Nov. 1964.
[47] D. D. Siljak, "Analysis and synthesis of feedback control systems in the parameter plane II-sampled-data systems," *IEEE Trans. Appl. Ind.*, vol. AI-83, no. 75, pp. 458–466, Nov. 1964.
[48] Y. P. Nikolaev, "The geometry of D-decomposition of a two-dimensional plane of arbitrary coefficients of the characteristic polynomial of a discrete system," *Autom. Remote Control*, vol. 65, no. 12, pp. 1904–1914, Dec. 2004.
[49] M. Shooman, "Stability analysis of nonlinear systems in the parameter plane," *IEEE Trans. Autom. Control*, vol. AC-9, no. 3, pp. 267–269, Jul. 1964.
[50] D. D. Siljak, "Analysis and synthesis of feedback control systems in the parameter plane III-nonlinear systems," *IEEE Trans. Appl. Ind.*, vol. AI-83, no. 75, pp. 466–473, Nov. 1964.
[51] E. N. Gryazina, B. T. Polyak, and A. A. Tremba, "D-decomposition technique state-of-the-art," *Autom. Remote Control*, vol. 69, no. 12, pp. 1991–2026, Dec. 2008.
[52] Y. I. Neimark, "D-partition and robust stability," *Comput. Math. Model.*, vol. 9, no. 2, pp. 160–166, Apr. 1998.
[53] A. A. Tremba, "Robust D-decomposition under l_p-bounded parametric uncertainties," *Autom. Remote Control*, vol. 67, no. 12, pp. 1878–1892, Dec. 2006.
[54] P. F. Pryashnikova, "Robust D-decomposition for a polynomial dependence of the coefficients of a polynomial on two parameters," *Autom. Remote Control*, vol. 83, no. 7, pp. 1078–1092, Jul. 2022.
[55] Z. Shafiei and A. T. Shenton, "Tuning of PID-type controllers for stable and unstable systems with time delay," *Automatica*, vol. 30, no. 10, pp. 1609–1615, Oct. 1994.
[56] Z. Shafiei and A. T. Shenton, "Frequency-domain design of PID controllers for stable and unstable systems with time delay," *Automatica*, vol. 33, no. 12, pp. 2223–2232, Dec. 1997.
[57] N. Hohenbichler, "All stabilizing PID controllers for time delay systems," *Automatica*, vol. 45, no. 11, pp. 2678–2684, Nov. 2009.

[58] P. D. Mandić, T. B. Šekara, M. P. Lazarević, and M. Bošković, "Dominant pole placement with fractional order PID controllers: D-decomposition approach," *ISA Trans.*, vol. 67, pp. 76–86, Mar. 2017.

[59] S. Elmadssia, K. Saadaoui, A. Zaguia, T. Ezzedine, and Q.-G. Wang, "Stabilization domains for second order delay systems," *IEEE Access*, vol. 9, pp. 53518–53529, 2021.

[60] B. T. Polyak and M. V. Khlebnikov, "New criteria for tuning PID controllers," *Autom. Remote Control*, vol. 83, no. 11, pp. 1724–1741, Nov. 2022.

[61] Wolfram Research. (2020). *Mathematica, Versions 13.1, 12.0*. [Online]. Available: https://www.wolfram.com/mathematica

[62] M. Henriksen and J. R. Isbell, "On the continuity of the real roots of an algebraic equation," *Proc. Amer. Math. Soc.*, vol. 4, no. 3, pp. 431–434, Jan. 1953.

[63] S. A. Broughton, "Continuous dependence of solutions of equations on parameters," Dept. Math., Rose-Hulman Inst. Technol., IN, USA, Tech. Rep. MSTR 14-03, Sep. 2014. [Online]. Available: http://www.rose-hulman.edu/math.aspx

CHYI HWANG received the B.Sc., M.Sc., and Ph.D. degrees from the Department of Chemical Engineering, National Cheng Kung University (NCKU), Taiwan, in 1976, 1978, and 1981, respectively.

From 1981 to 1993, he was a Faculty Member with the Department of Chemical Engineering, NCKU. In 1993, he joined the Department of Chemical Engineering, National Chung Cheng University, and the Department Chair, from 1993 to 1999. In 2004, he was recruited to I-Shou University, Kaohsiung, Taiwan, where he was appointed as a University Chair Professor. From 2007 to 2014, he was the Dean of Academic Affairs. From 2014 to 2017, he was appointed by the Ministry of Education, Taiwan, as the President of National Quemoy University. Currently, he is with National Chung Cheng University as a specially appointed Researcher with the honor of a Chair Professor. He is interested in systems and control theory, optimization techniques, and computational methods. He has coauthored more than 200 journal articles. He received the Outstanding Special Researcher Award from the National Science Council of ROC, in 2002.

TZU-CHI WANG received the B.Sc. degree from the Department of Chemical Engineering, Chinese Culture University, in 1994, the M.Sc. degree from the Department of Chemical Engineering, National Chung Cheng University, in 1996, and the Ph.D. degree from the Department of Chemical Engineering, National Taiwan University, in 2000.

From 2000 to 2005, he was with Green Energy and Environment Research Laboratories (ITRI). In 2005, he joined the Department of Chemical and Materials Engineering, Chinese Culture University, where he became a Professor, in 2015. From 2012 to 2022, he was elected as the Department Chair. In 2021, he was the Dean of the Research and Development Department of the University. He has been the President of the University, since 2022. He is interested in program design, quantitative risk analysis, control theory, and industry process control. He has co-published more than 100 journal articles and seminar papers with others. He is the Chairperson of Taiwan Occupational Safety Society.

FENG-SHENG WANG received the Ph.D. degree in chemical engineering from the National Taiwan University of Science and Technology, in 1986. Subsequently, he was a Faculty Member with the Department of Chemical Engineering, Feng Chia University, Taichung, Taiwan, from 1986 to 1990. Currently, he is a Professor with the Department of Chemical Engineering, National Cheng Chung University, Chiayi City, Taiwan. His research interests include hybrid differential evolution, constraint-based modeling, and cancer metabolism.

LI-SHIN LU received the B.Sc. degree in mechanical engineering from Tamkang University, New Taipei City, Taiwan, in 1994, and the M.Sc. and Ph.D. degrees in mechanical engineering from National Central University, Taoyuan, Taiwan, in 1996 and 2006, respectively. He is currently an Associate Professor with the Department of Industrial Engineering and Management, National Quemoy University, Kinmen, Taiwan. His current research interests include automatic control, semiconductor manufacturing, and powder technology.